

## Prompt neutron emission from the spontaneous fission of $^{260}\text{Md}$

J. F. Wild,<sup>(a)</sup> J. van Aarle,<sup>(a),(b)</sup> W. Westmeier,<sup>(b)</sup> R. W. Lougheed,<sup>(a)</sup> E. K. Hulet,<sup>(a)</sup> K. J. Moody,<sup>(a)</sup> R. J. Dougan,<sup>(a)</sup>  
E.-A. Koop,<sup>(b)</sup> R. E. Glaser,<sup>(a)</sup> R. Brandt,<sup>(b)</sup> and P. Patzelt,<sup>(b)</sup>

<sup>(a)</sup>University of California, Lawrence Livermore National Laboratory, Livermore, California 94551

<sup>(b)</sup>Philipps University, D-3550, Marburg an der Lahn, Federal Republic of Germany

(Received 7 June 1989)

We have made the first measurement of the number of neutrons emitted from the spontaneous fission of a nuclide in which very high fragment energies dominate the fission process. In bombardments of  $^{254}\text{Es}$ , we produced a large sample of 28-d  $^{260}\text{Md}$ , which was neutron counted in a 1-m-diameter spherical tank containing a Gd-doped scintillator solution. The average number of neutrons emitted per fission is only  $2.58 \pm 0.11$ , substantially less than for other actinides. A linear dependence of neutron multiplicity on fragment-excitation energy is observed to the highest values of total kinetic energy.

### I. INTRODUCTION

The spontaneous fission (SF) of 28-d  $^{260}\text{Md}$  has been shown to be markedly bimodal;<sup>1,2</sup> about 60% of the fissions have total kinetic energies (TKE) in an approximately Gaussian distribution peaking at 235 MeV, with the remainder in a distribution peaking at about 200 MeV (see Fig. 1). These fission properties are unusual and are remarkably different from those of lighter actinides. The high-TKE fission mode arises from the existence of nearly spherical fragments with atomic numbers and masses near those of the doubly magic nucleus  $^{132}\text{Sn}$ . The mass distribution is sharply symmetric, with a full width at half maximum of only 8 u. On the other hand, the low-TKE fission mode arises from elongated scission shapes in which the fragments are highly deformed; the mass distribution for this mode of SF is also symmetric, but the width of the distribution is several times greater than that for the high-TKE mode. At scission, varying amounts of potential energy are associated with the fragments, depending upon the degree of deformation they possess; following scission, this potential energy of deformation is converted rapidly to internal excitation energy. There is a direct relationship between the degree of fragment deformation at scission and the amount of fragment excitation energy.

In nuclear fission, the fragment excitation energy, originating mostly from deformation energy, is part of the total energy released in the fission process. The total energy release is determined by the mass difference between the fissioning species and the fragments and is known as the  $Q$  value for fission. The major part of this total energy is given up as kinetic energy of the fragments; the remainder exists in the form of fragment excitation energy and is dissipated mainly through the emission of gamma rays and the evaporation of prompt neutrons. The number of prompt neutrons emitted in a fission event is related directly to the excitation energy of the fragments<sup>3</sup> and is, therefore, a measure of the deformation of the fragments at scission.

To this point, neutron emission in spontaneous fission has been studied for nuclides undergoing SF with only asymmetric mass distributions and average TKE values described by the systematics of Unik *et al.*<sup>4</sup> and Viola *et al.*<sup>5</sup> Until  $^{258}\text{Fm}$  is reached, this "standard" fission is characterized by modest increases in TKE, the number of neutrons emitted, and fission  $Q$  values with increasing  $Z$  of the fissioning species. The SF-emitting nuclide  $^{260}\text{Md}$  offers the first good test of the relationship of neutron emission and fragment excitation in the regime of low fragment-excitation energies. With its long half-life (enabling a source to be prepared and sent to the experiment), the relative ease of production (thousand of atoms), and the large proportion of high-TKE fission events,  $^{260}\text{Md}$  offered us an opportunity to study neutron emission from a fission system uniquely different from those otherwise encountered in this region of nuclides. Therefore, we have measured in coincidence the prompt neutron emission and the fragment energies and masses associated with the SF of  $^{260}\text{Md}$ . We felt that the results would test strongly the correlation between fragment kinetic energy, fragment deformation, and neutron-emission probability over a range of values wider than ever before.

### II. EXPERIMENTAL

The  $^{260}\text{Md}$  used in this experiment was produced by the bombardment of 276-d  $^{254}\text{Es}$  with 126-MeV  $^{22}\text{Ne}$  ions at the 88-inch cyclotron of the Lawrence Berkeley Laboratory. In a two-and-one-half month period, we made 34 bombardments, ranging in duration from about 90 min to 8 h, as part of another experiment; for each bombardment, we collected products recoiling from the Es target onto a thin, Mo foil and performed chemical separations on each foil immediately after the end of bombardment. The Md fraction from each bombardment was set aside; later, these fractions were combined and purified extensively through the use of ion-exchange chromatography. The  $^{260}\text{Md}$ , amounting to about 3000 atoms, was electro-

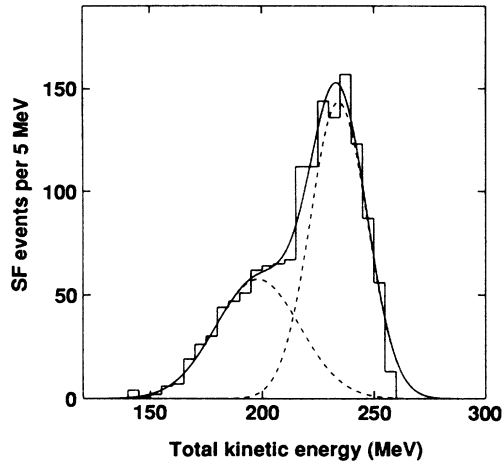


FIG. 1. The TKE distribution for  $^{260}\text{Md}$  SF obtained from this experiment and a previous work. The two dashed Gaussian curves represent the low- and high-TKE regions of bimodal fission; the high-TKE region contains approximately 63% of the events.

plated on a thin ( $27 \mu\text{g}/\text{cm}^2$ ) polyimide film which had previously been overcoated with  $25 \mu\text{g}/\text{cm}^2$  of Au and which was supported by a metal ring. The sample was then sent to Philipps University, Marburg, FRG, for the neutron multiplicity measurement.

The neutron counter<sup>6</sup> is a sphere with an outer diameter of 1.06 m; a 12-cm-diameter cylindrical opening through the center of the sphere contains an evacuated chamber for the sample and opposing surface-barrier detectors for the measurement of coincident fragment energies. The surrounding volume inside the sphere contains the scintillator solution NE 323, a toluene-based mixture containing about 0.5 weight percent of Gd. Fission neutrons emitted into the sphere are thermalized in the organic solvent; they are subsequently captured by the Gd with the emission of capture gamma rays. The scintillator material in the solution is stimulated by the gamma rays to emit light at the violet end of the visible

spectrum. To detect these light pulses, twelve photomultiplier tubes are mounted on the outer surface of the counter at approximately the positions of the faces of a dodecahedron. The inner surface of the counter is coated with titanium dioxide to minimize the absorption of the light by the counter walls.

A diagram of the pulse-processing modules is shown in Fig. 2. The detection of a signal from the linear amplifier of either surface-barrier detector opened a  $35\text{-}\mu\text{s}$  gate after a  $0.5\text{-}\mu\text{s}$  delay designed to exclude prompt gamma rays or proton-recoil pulses. The photomultiplier tubes were given alternately even and odd numbers; in order for the detection of a neutron to be considered valid, coincident pulses were required from at least two adjacent photomultiplier tubes (one even, one odd) during the  $35\text{-}\mu\text{s}$  period that the gate was open (note that the recording of a neutron signal was not necessary to validate a fission event). Neutron signals acquired during a fission event were counted by a scaler while the  $35\text{-}\mu\text{s}$  gate was open. The collected fragment-energy pulses and the number of absorbed neutrons from each SF event were passed to a multichannel analyzer for digitization and storage.

The surface-barrier detectors were calibrated with a standard source of  $^{252}\text{Cf}$  prepared in a manner identical to that of the  $^{260}\text{Md}$  source. Pulse-height defect corrections to the fragment energies were made with the parameters of Weissenberger *et al.*<sup>7</sup> All fragment masses and kinetic energies derived from this calibration are provisional (no neutron-emission correction) unless otherwise indicated. For our calibrations, we adopted the neutron distribution parameters given by Spencer *et al.*<sup>8</sup> for  $^{252}\text{Cf}$ , such as  $\bar{\nu}_T$  and the distribution variance. Although Axton<sup>9</sup> analyzed thoroughly the literature values for  $\bar{\nu}_T$  for  $^{252}\text{Cf}$ , arriving at a representative average of  $3.766 \pm 0.005$ , he gave no individual multiplicity values. Spencer gave a value of  $3.773 \pm 0.007$  for  $\bar{\nu}_T$  in agreement with Axton, and also presented individual multiplicity values. Raw neutron-counting data were corrected for the effects of counter background, dead time, and

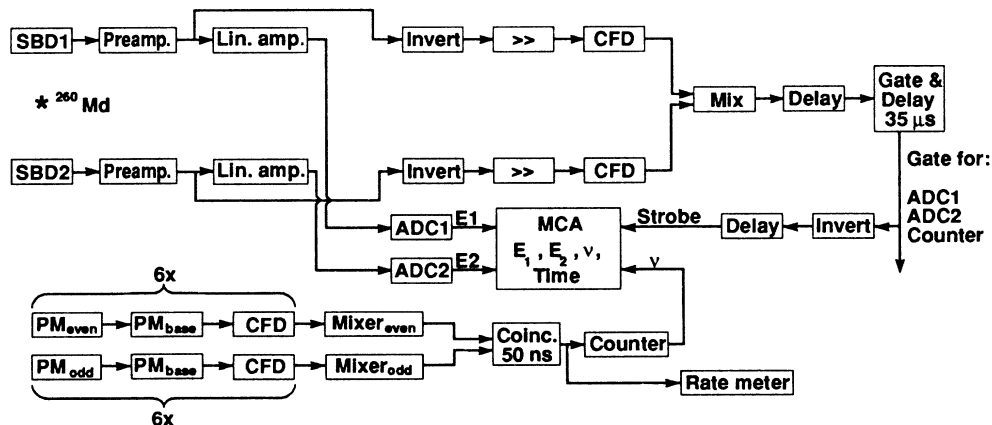


FIG. 2. The electronic setup used to measure both the neutron emission and fragment kinetic energies from the SF of  $^{260}\text{Md}$  in this experiment.

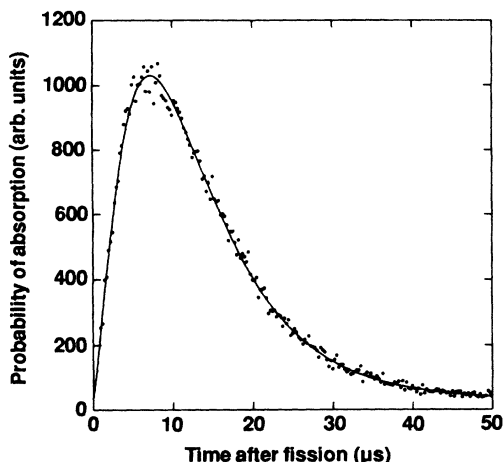


FIG. 3. The relative probability of neutron capture as a function of time after the fission event determined for the neutron counter used in this experiment.

efficiency using the method described by Ribrag *et al.*<sup>10</sup> and adopted by Spencer *et al.*<sup>8</sup> the solution of simultaneous linear equations by the matrix inversion technique.

#### A. Background correction

The neutron background rate was determined by opening a 35- $\mu$ s gate twice every 500 s during the counting of the sample. The average number of background counts per gate was  $0.164 \pm 0.002$  for over 33 000 gates; the multiplicity distribution is well described by a Poisson distribution. The background correction was made using the following equation:

$$\{M\} = [B]^{-1}\{N\}, \quad (1)$$

where  $\{M\}$  is the column vector containing the measured multiplicity distribution;  $[B]$  is a square matrix whose elements  $b_{i,j}$  are the probabilities of counting  $i$  events (including background) given that among these,  $j$  neutrons were counted ( $i \geq j$ ); and  $\{N\}$  is the column vector containing the background-corrected distribution (the probability of counting  $j$  neutrons).

#### B. Counter dead-time correction

After each pulse, the scaler used to count neutrons from each fission event was dead for 0.84  $\mu$ s, which is quite a large fraction of the time the 35- $\mu$ s gate was open, especially for higher multiplicity events. Therefore, it was necessary to make this correction as precisely as possible, because the fraction of events lost due to dead time increases approximately as the power of the multiplicity. For this reason, we remeasured the function relating the probability of the capture of a neutron as a function of the time after the fission event for this instrument. This was done by counting the  $^{252}\text{Cf}$  source and allowing the detection of a fission fragment in one of the surface-barrier detectors to serve as a start signal, which then opened a 0.5- $\mu$ s gate at a known random time within a 60- $\mu$ s time interval generated by a precision pulser. The

number of times neutrons were detected in each specific time interval was recorded with a multichannel analyzer. The resulting probability of neutron capture by the instrument as a function of time after the fission event is shown in Fig. 3. After a flat background was subtracted, this curve was fitted by the method of least squares to the function<sup>8</sup>

$$f(t) = A(e^{-\beta t} - e^{-\lambda t}) - Bte^{-\lambda t}, \quad (2)$$

where  $A$ ,  $B$ ,  $\beta$ , and  $\lambda$  are adjustable parameters. Integration of the above function over the 35- $\mu$ s gate period indicated that 96.1% of the neutrons would be captured while the gate was open.

The dead-time correction was made using the following equation:

$$\{N\} = [S]^{-1}\{D\}, \quad (3)$$

where  $\{N\}$  is defined as in Eq. (1);  $[S]$  is a square matrix whose elements  $s_{i,j}$  are the probabilities of counting  $i$  neutrons given that  $j$  neutrons were captured within the 35  $\mu$ s that the counting window was open (i.e., not observing  $j-i$  neutrons due to dead-time losses;  $i \leq j$ ); and  $\{D\}$  is the column vector containing the dead-time-corrected distribution (the probability that  $j$  neutrons were within the counting window).

The calculation of the matrix elements  $s_{i,j}$  according to the equations given in Ref. 8 becomes rapidly overwhelming even for low multiplicity values. Therefore, we determined the matrix coefficients necessary to correct our data for the effects of dead time by the Monte Carlo method using the cumulative distribution function of Eq. (2) to predict the fraction of neutron signals lost while the system was dead.

#### C. Counter-efficiency correction

Finally, the correction for counter efficiency, defined as the probability that any given neutron is captured and emits a signal during the period that the 35- $\mu$ s window is open, was made in a manner similar to that of the background and dead-time corrections; the following equation was used to make the efficiency correction:

$$\{D\} = [P]^{-1}\{v\}, \quad (4)$$

where  $\{D\}$  is described following Eq. (3);  $[P]$  is a square matrix whose elements  $p_{i,j}$  are the probabilities that  $i$  neutrons have been absorbed within the gate period given that  $j$  neutrons are emitted; and  $\{v\}$  is the column vector containing the efficiency-corrected distribution (the probability that  $j$  neutrons are emitted). The values for the matrix elements  $p_{i,j}$  are obtained from the binomial distribution function as follows:

$$p_{i,j} = \binom{j}{i} \epsilon^i (1-\epsilon)^{j-i}, \quad (5)$$

where  $\epsilon$  is the efficiency.

The neutron-detection efficiency of the scintillator tank was determined by normalizing neutron multiplicity data from the  $^{252}\text{Cf}$  standard, corrected for background and dead time, to give an average of 3.773 neutrons per fission

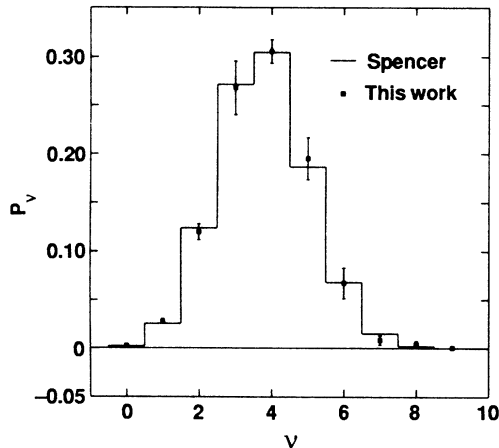


FIG. 4. A comparison of the  $^{252}\text{Cf}$  neutron-multiplicity distribution obtained in this work to calibrate the neutron counter efficiency (square data points) with that from Spencer *et al.* (Ref. 8) (histogram).

as determined in Ref. 8. The value for the efficiency that we obtained in this manner was 102%. It is very obvious that this number cannot represent just the actual probability for detecting a neutron. Even with the large size of our scintillator tank, we would expect the actual detection efficiency to be no more than 95%; the efficiency should have an upper limit of 96.1%, the fraction of neutrons that are captured within the 35- $\mu\text{s}$  gate period. However, a comparison of the corrected neutron-multiplicity distribution for  $^{252}\text{Cf}$  from our neutron counter (34 257 events) and from Ref. 8 (shown in Table I and graphed in Fig. 4) indicates that we must have made the background, dead-time, and efficiency corrections properly. Had we not done so, we could not have matched so well the average multiplicity, the multiplicity distribution, and the “invariant  $R$ ” ( $R_{\text{inv}}$ ) for  $^{252}\text{Cf}$ , as measured by Spencer *et al.*<sup>8</sup> This parameter is indepen-

TABLE I. Comparison of neutron-emission probabilities for  $^{252}\text{Cf}$  from this work and from Ref. 8.

$\nu$	This work	Reference 8
0	$0.0025 \pm 0.0004$	$0.0022 \pm 0.0001$
1	$0.0282 \pm 0.0024$	$0.0256 \pm 0.0013$
2	$0.1199 \pm 0.0081$	$0.1239 \pm 0.0014$
3	$0.2681 \pm 0.0278$	$0.2715 \pm 0.0011$
4	$0.3056 \pm 0.0118$	$0.3046 \pm 0.0005$
5	$0.1951 \pm 0.0217$	$0.1866 \pm 0.0006$
6	$0.0674 \pm 0.0158$	$0.0681 \pm 0.0004$
7	$0.0084 \pm 0.0048$	$0.0152 \pm 0.0001$
8	$0.0045 \pm 0.0030$	$0.0021 \pm 0.0000$
9	$0.0004 \pm 0.0015$	$0.0002 \pm 0.0000$
Avg.	$3.773 \pm 0.111$	$3.773 \pm 0.007$
Variance	$1.612 \pm 0.141$	1.6155
$R_{\text{inv}}^a$	$-0.1518 \pm 0.0011$	$-0.1517 \pm 0.0001$

<sup>a</sup>The “invariant  $R$ ,” assumed to be independent of counter efficiency (Refs. 3, 8, and 10).

dent of detection efficiency but is strongly dependent upon the dead-time correction.<sup>10,3</sup>

Because of the large dead time of 0.84  $\mu\text{s}$  per neutron pulse, and perhaps because of the correction method used, we believe the multiplicity distribution might be overcorrected for dead time. This means that the average multiplicity and distribution variance were raised to values higher than they should have been, to values greater than the  $^{252}\text{Cf}$  target values, and that the multiplicity distribution had to be undercorrected for efficiency (average multiplicity and variance reduced) to achieve the “true” multiplicity distribution. This can only occur if the “efficiency” is greater than 100%. The combination of these two corrections, however, yielded the proper multiplicity distribution for  $^{252}\text{Cf}$  and gave us the confidence to use these same correction methods to unfold the observed neutron multiplicity distribution for  $^{260}\text{Md}$ .

We also examined the effect of various parametric uncertainties on our values of  $\bar{\nu}_T$ , distribution variance, and individual multiplicities. We did this by expanding the matrix equation for neutron multiplicity as determined from the raw counting data [Eq. (6), below]

$$\{\nu\} = [P]^{-1}[S]^{-1}[B]^{-1}\{M\} \quad (6)$$

in a Taylor series and approximating from this expression the variances of these components as functions of the variance and covariance of other parameters. The uncertainty in the detection efficiency was found to have the greatest effect on the parameters we measured. Due to the higher multiplicity of neutrons from the SF of  $^{252}\text{Cf}$ , the effect of uncertainties on corrections was larger (because the corrections were larger) than for  $^{260}\text{Md}$ , where half of the SF events have multiplicities of two or fewer and require less correction of the raw counting data.

### III. RESULTS AND DISCUSSION

In 98 d of counting, we obtained 1207 fission events, all of which were used to determine the neutron-multiplicity distribution. The corrected (true) neutron-multiplicity distribution for  $^{260}\text{Md}$  is shown in Fig. 5 and is compared in Table II with that of  $^{257}\text{Fm}$ , the heaviest nuclide for which a neutron-multiplicity distribution had previously been measured.<sup>11</sup> The average multiplicity is  $2.58 \pm 0.11$  neutrons per fission for  $^{260}\text{Md}$ , more than one neutron per fission lower than that of other nuclides in the heavy actinide region for which neutron measurements have been made.<sup>11</sup> More than 25% of the SF events from  $^{260}\text{Md}$  emit fewer than two neutrons; in comparison, only about 8% of  $^{257}\text{Fm}$  fissions and 3% of  $^{252}\text{Cf}$  fissions (see Table I) emit fewer than two neutrons. The distribution variance,  $2.57 \pm 0.13$ , is considerably higher than that of  $^{252}\text{Cf}$  (1.62), due to summing the breadths of the individual distributions from the two modes of fission of  $^{260}\text{Md}$ .

For 905 events, energies from both fragments were also recorded, enabling us to correlate neutron emission with the kinetic energy of the fissioning system. In Fig. 6, we show two partial neutron-multiplicity distributions for  $^{260}\text{Md}$ . The dashed histogram with the triangular data points was obtained from SF events with TKE values

TABLE II. Comparison of neutron-emission probabilities for  $^{260}\text{Md}$  and for  $^{257}\text{Fm}$  (Ref. 11).

$\nu$	$^{260}\text{Md}$	$^{257}\text{Fm}$
0	$0.091 \pm 0.009$	$0.022 \pm 0.003$
1	$0.180 \pm 0.013$	$0.058 \pm 0.004$
2	$0.250 \pm 0.018$	$0.127 \pm 0.004$
3	$0.192 \pm 0.033$	$0.210 \pm 0.005$
4	$0.163 \pm 0.024$	$0.259 \pm 0.006$
5	$0.083 \pm 0.031$	$0.190 \pm 0.006$
6	$0.022 \pm 0.026$	$0.095 \pm 0.004$
7	$0.023 \pm 0.014$	$0.030 \pm 0.003$
8	$-0.004 \pm 0.002$	$0.007 \pm 0.002$
9	$0.000 \pm 0.001$	$0.002 \pm 0.002$
Avg.	$2.58 \pm 0.11$	$3.779 \pm 0.005^a$
Variance	$2.57 \pm 0.13$	$2.54 \pm 0.11$

<sup>a</sup>Renormalized from value of 3.769 in Ref. 11 to reflect value of  $\bar{\nu}_T$  for  $^{252}\text{Cf}$  of 3.773.

exceeding 224 MeV (53% of the distribution). These events represent a major portion of the high-TKE mode of bimodal fission and possess a symmetric, sharply peaked mass distribution (see the dotted histogram in Fig. 7). They have an average emission rate of  $1.58 \pm 0.10$  neutrons per fission; such a low rate implies that there cannot be much fragment excitation energy, and, therefore, at scission these fragments must be nearly spherical. The solid histogram with the square data points in Fig. 6 was sorted from fission events with TKE values less than 210 MeV (29% of the distribution). This group of fission events represents the low-TKE mode of bimodal fission, and its mass distribution, although still symmetric, is much broader than that of the high-TKE mode (see the solid histogram in Fig. 7). With an average emission of  $4.17 \pm 0.15$  neutrons per fission this group of fission events is more typical of "conventional" SF from the

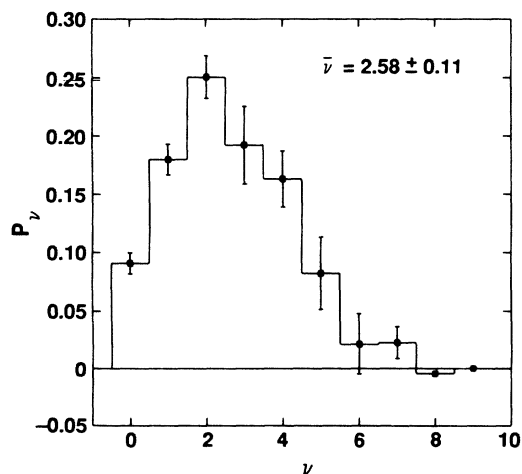


FIG. 5. The total neutron-multiplicity distribution from the SF of  $^{260}\text{Md}$ , corrected for background, dead time, and counter efficiency. The average multiplicity is  $2.58 \pm 0.11$  neutrons per fission.

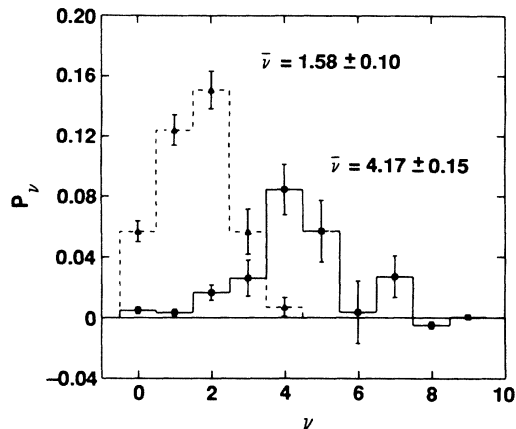


FIG. 6. Partial neutron-multiplicity distributions from the SF of  $^{260}\text{Md}$ ; the dashed histogram (triangular data points) is derived from fission events with  $\text{TKE} \geq 224$  MeV (upper 53% of TKE distribution); the solid histogram (square data points) was obtained from fission events with  $\text{TKE} \leq 210$  MeV (lower 29% of the TKE distribution).

heavier actinides such as  $^{252}\text{Cf}$ . This emission rate requires substantially more excitation energy from the fragments, indicating the presence of considerably more fragment deformation and an elongated scission shape.

As further evidence that the number of neutrons per fission is related to fragment excitation energy, we can estimate the fragment excitation energy ( $E^*$ ) for fission by calculating the mass-weighted average  $Q$  value for a given range of total kinetic energies and subtracting from it the measured average TKE for events in the same energy range. We did this for several ranges of TKE from the SF of  $^{260}\text{Md}$ ; the mass excess values for the fission products were obtained from the calculations of Comay *et al.*,<sup>12</sup> we also used this compilation to estimate the mass of  $^{260}\text{Md}$  in order to maintain consistency. We obtained a value of +96.04 MeV for the  $^{260}\text{Md}$  mass excess from a linear extrapolation of the Comay *et al.* mass excesses

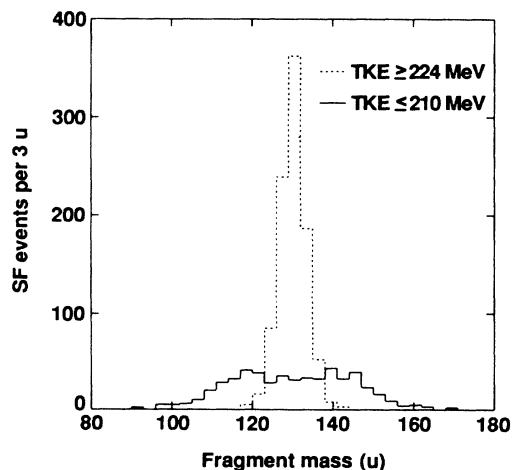


FIG. 7. Partial mass distributions obtained from the SF of  $^{260}\text{Md}$  for events with  $\text{TKE} \geq 224$  MeV (dotted histogram) and for events with  $\text{TKE} \leq 210$  MeV (solid histogram).

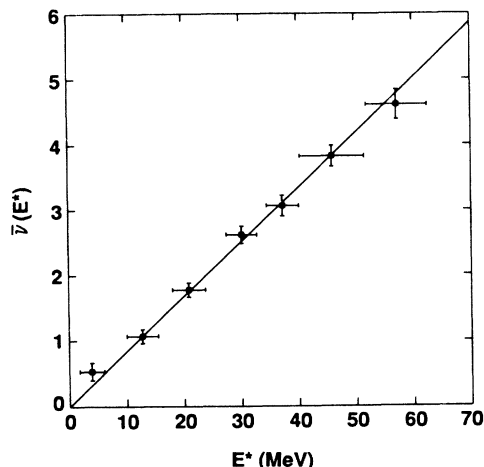


FIG. 8. A plot of  $\bar{\nu}$  vs  $E^*$  (fragment-excitation energy) for the SF of  $^{260}\text{Md}$  showing the linear relationship between available fragment-excitation energy and neutron emission. The solid line was determined by least-squares fitting.

for nearby even- $A$  Md isotopes. In Fig. 8 we have plotted  $E^*$  vs the average number of neutrons emitted by fissions in each energy range. The strong linear correlation between average neutron multiplicity and  $E^*$  demonstrates that neutron emission is directly related to fragment-excitation energy, and, for events with very low values of  $E^*$ , less than even one neutron per fission can be emitted on the average.

The average energy required to emit the next neutron from a fission fragment from  $^{260}\text{Md}$  can be estimated from the data shown in Fig. 9, the number of neutrons emitted as a function of TKE, using the estimation method of Nifenecker *et al.*<sup>3</sup> According to this method, this average energy can be obtained from the product of the inverse of the slope from Fig. 9 and a ratio of variances of TKE distributions: the ratio of the average variance of TKE for a given mass division and the variance

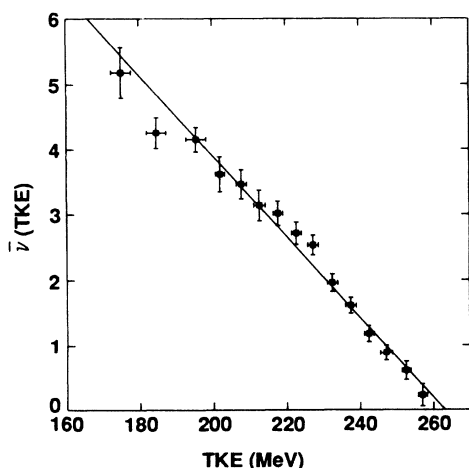


FIG. 9. A plot of  $\bar{\nu}$  vs TKE for the SF of  $^{260}\text{Md}$ , showing the linearity of the relationship even to the highest values of TKE. The solid line was determined by least-squares fitting and corresponds to a value of  $16.2 \pm 0.7$  MeV per neutron.

for the entire TKE distribution. The inverse of the slope of the line in Fig. 9 is  $16.2 \pm 0.7$  MeV per neutron. For events with masses between 110 and 150 (more than 95% of the distribution), the average variance of the TKE distribution for SF events with a given mass division is  $244.1 \text{ MeV}^2$  (MeV squared), while for the overall TKE distribution between masses 110 and 150 it is  $438.5 \text{ MeV}^2$ . From these parameters, we calculate an average value of  $9.0 \pm 0.4$  MeV needed to emit the next neutron, this energy consisting principally of the average neutron binding energy and the center-of-mass kinetic energy. As expected, this value is greater than the 8.6 MeV/neutron obtained for  $^{252}\text{Cf}$  by Nifenecker *et al.*,<sup>3</sup> because on the average the  $^{260}\text{Md}$  fragments are more spherical, are closer to closed nucleon shells, and, therefore, have higher average neutron binding energies. If we choose events with masses between 120 and 140 (still over 80% of the total), we obtain a value of 11.8 MeV for the energy needed to emit the next neutron. This is in line with the data of Nifenecker *et al.*,<sup>3</sup> who show in their Fig. 5 experimentally measured values of energy carried away per neutron as a function of fragment mass for  $^{252}\text{Cf}$  SF. It can be seen that for events in the mass-symmetric region, values of about 12 MeV per neutron have been obtained.

Our data provide us only the sum of the neutrons emitted from the fragments as a function of mass division. We must assume in some way the contribution from each fragment for a given mass division in order to generate the function  $\bar{\nu}(M)$  vs fragment mass. To do this, we obtained a calculation made by Brosa<sup>13</sup> of this function for  $^{260}\text{Md}$  and used it to partition our measured neutron emission between the fragments. The resulting sawtooth curve differs in shape somewhat from Brosa's calculated  $\bar{\nu}(M)$  curve. We compare the two in Fig. 10; the line drawn through our data points represents an "eyeball" fit, and the dotted curve is Brosa's unnormalized calculation. The calculation overestimates the neutron emission

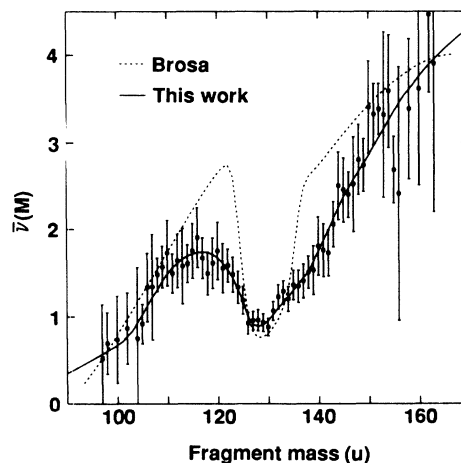


FIG. 10. The function  $\bar{\nu}(M)$  vs fragment mass derived for  $^{260}\text{Md}$  SF, with our measured values for total neutron emission for a given mass division partitioned between the fragments according to the calculation of Brosa (Ref. 13). The dotted curve is Brosa's calculated function (unnormalized), while the solid curve is an "eyeball" estimate of the fit through the data points.

for fragments with masses 115–125 and 135–145 but reproduces quite well that of symmetric mass division. When coupled with our mass distribution, the calculation yields an average emission rate of 3.0 neutrons per fission.

We expect the effect of neutron emission on the fragment energies and masses to be less for the SF of  $^{260}\text{Md}$  than for the SF of  $^{252}\text{Cf}$ . The majority of  $^{260}\text{Md}$  fragments have masses within 5 u of mass symmetry where, as shown in Fig. 10, only about one neutron is emitted per fragment. In the case of  $^{252}\text{Cf}$ , the majority of fragments emit about two neutrons each, resulting in a larger correction from provisional mass and energy values.

In summary, we have shown that the lower average neutron multiplicity from the SF of  $^{260}\text{Md}$  indeed results from the lower average excitation energy of the fragments because the high-TKE fission mode has nearly spherical fragments. We have extended this relationship

between excitation energy and number of neutrons emitted over a much broader range than in previous experiments.

#### ACKNOWLEDGEMENTS

The authors are indebted for the use of the  $^{254}\text{Es}$  target material to the Office of Basic Energy Sciences, U. S. Department of Energy, through the transplutonium element production facilities of the Oak Ridge National Laboratory. This work was performed under the auspices of the U. S. Department of Energy by the Lawrence Livermore National Laboratory under Contract No. W-7405-ENG-48 and was also supported by the Federal Republic of Germany Bundesministerium für Forschung und Technologie under Contract No. 06MR553.

<sup>1</sup>E. K. Hulet, J. F. Wild, R. J. Dougan, R. W. Lougheed, J. H. Landrum, A. D. Dougan, M. Schädel, R. L. Hahn, P. A. Baisden, C. M. Henderson, R. J. Dupzyk, K. Sümmerer, and G. R. Bethune, *Phys. Rev. Lett.* **56**, 313 (1986).

<sup>2</sup>E. K. Hulet *et al.*, *Phys. Rev. C* **40**, 770 (1989).

<sup>3</sup>H. Nifenecker, C. Signarbieux, R. Babinet, and J. Poitou, in *Proceedings of the International Symposium on the Physics and Chemistry of Fission, Rochester, 1973* (IAEA, Vienna, 1974), Vol. II, p. 117.

<sup>4</sup>J. P. Unik, J. E. Gindler, L. E. Glendenin, K. F. Flynn, A. Gorski, and R. K. Sjöblom, in *Proceedings of the International Symposium on the Physics and Chemistry of Fission, Rochester, 1973* (IAEA, Vienna, 1974), Vol. II, p. 19.

<sup>5</sup>V. E. Viola, K. Kwiatkowski, and M. Walker, *Phys. Rev. C* **31**, 1550 (1985).

<sup>6</sup>E.-A. Koop, Dr. rer. nat. thesis, Phillips University, 1986.

<sup>7</sup>E. Weissenberger, P. Geltenbort, A. Oed, F. Gönnerwein, and H. Faust, *Nucl. Instrum. Methods* **A248**, 506 (1986).

<sup>8</sup>R. R. Spencer, R. Gwin, and R. Ingle, *Nucl. Sci. Eng.* **80**, 603 (1982).

<sup>9</sup>E. J. Axton, *Eur. Appl. Res. Rep.—Nucl. Sci. Technol.* **5**, 609 (1984).

<sup>10</sup>M. Ribrag, J. Poitou, J. Matusek, and C. Signarbieux, *Rev. Phys. Appl* **7**, 197 (1972).

<sup>11</sup>D. C. Hoffman, G. P. Ford, J. P. Balagna, and L. R. Veaser, *Phys. Rev. C* **21**, 637 (1980).

<sup>12</sup>E. Comay, I. Kelson, and A. Zidon, *At. Data Nucl. Data Tables* **39**, 235 (1988).

<sup>13</sup>U. Brosa (private communication).